



# WEDNESDAY SLIDE CONFERENCE 2024-2025

Conference #13

04 December 2024

## CASE I:

### **Signalment:**

20-year-old, male, African lion, *Panthera leo*, Felidae.

### **History:**

This lion had a clinical picture characterized by mild bleeding in the oral cavity, which lasted approximately for two weeks, and had been associated with an increase of the volume of the mandible. After this time, hemorrhagic episodes were observed sporadically.

### **Gross Pathology:**

During the examination of the mandible, there was a firm, irregular mass, approximately 3.0 cm in length, with white areas interspersed with yellow foci located in the mandibula at the height of the lower left canine. Dental mobility of mandibular canines and a fracture of the mandibular bone, near to the mental protuberance were noted.

### **Microscopic Description:**

Histopathology of the mandible revealed a non-encapsulated, expansive and infiltrative mass consisting of markedly pleomorphic keratinocytes, arranged either in mantles or in solid nests, supported by moderate to large fibrovascular stroma. In the center of some of these nests, deposition of lamellar eosinophilic material (keratin pearls) was noted and, occasionally, individual keratinocytes exhibited dyskeratosis. These cells have polygonal contours, moderate to broad cytoplasm,



**Figure 1-1. Mandible, lion. Within the fractured mandible, there is a 3cm firm, irregular mass. (Photo courtesy of: Federal Rural University of Pernambuco, [www.ufrpe.br](http://www.ufrpe.br))**

slightly eosinophilic, and round to oval vesicular nuclei with loose chromatin and 1 to 2 evident nucleoli. Moderate anisocytosis, anisokaryosis, and multifocal areas of intratumoral necrosis are noted. Mitotic counts are 2-4 mitosis per higher magnification field (40X).

### **Contributor's Morphologic Diagnosis:**

Well-differentiated squamous cell carcinoma.

### **Contributor's Comment:**

Squamous cell carcinoma (SCC) is one of the main oral cavity tumors in domestic cats and may represent more than 60% of all oral tumors in this species.<sup>1</sup> In wild felids however,

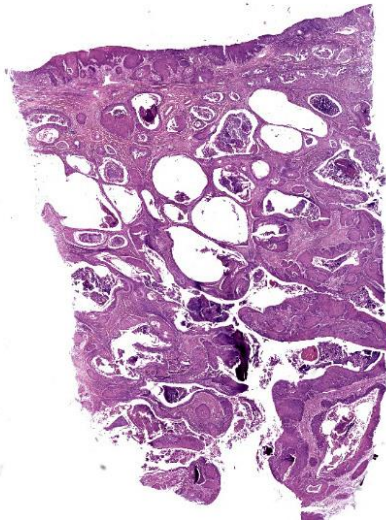


**Figure 1-2. Mandible, lion. One section of mandibular mucosa is submitted for examination. Extending downward from the mucosa, there are numerous islands and trabeculae of neoplastic keratinizing squamous epithelium. (HE, 5X)**

its description is sporadic and current records include tumors affecting the oral cavity of lynxes and ocelots,<sup>2-4</sup> the ear of leopards,<sup>5,6</sup> the eyelid region of white tigers,<sup>7,8</sup> the jaw of a Siberian tiger,<sup>9</sup> and the leopard right hind limb.<sup>10</sup> In *Panthera* sp. the diagnosis of SCC is better described in the snow leopard (*P. uncia*),<sup>11</sup> in which cutaneous and oral SCCs can represent up to 9% of the causes of death.<sup>12</sup>

The high frequency of papillomas and oral SCCs associated with the isolation of papillomaviruses in *P. uncia* strengthens the hypothesis of the participation of viruses in the etiology of SCC in large felids.<sup>12,15,16,20</sup> Other potential factors that may be related to carcinogenesis of oral SCC in these animals include pollution of urban centers<sup>9</sup> as well previous dental diseases.<sup>17,18</sup> In large felids, the upper and lower incisors seem to show a tendency for periodontal disease<sup>17,18</sup> and are common sites of neoplasm growth in lions.<sup>9,19,20</sup> It is important to highlight that the captive environment can influence the

formation of calculi and periodontal diseases in tigers and lions as compared to free-living species,<sup>18</sup> which can favor the formation of pre-neoplastic lesions.

The tongue and mandible seem to be important anatomical sites for SCCs in large felids, appearing as masses of rapid growth that are generally ulcerated and hemorrhagic with progressively infiltrative behavior. Microscopically, features such as the formation of keratin beads and individual keratinization of keratinocytes favored the diagnosis of SCC, considering that they are classic findings of neoplasia in well-differentiated to moderately-differentiated cases. Tumor expansiveness even favored bony lysis and cutaneous fistulation as identified in this case, whose clinical progression, degree of metastasis and evolution to death tend to be quite variable between species.

As there are few reports in the literature on wild felids, there is no definitive parameter on the survival time in cases of oral SCC in these animals. In domestic cats, neither the size of the mass nor its location in the mouth seem to be associated with survival time.<sup>21</sup> Important differential diagnoses in lions include potential oral cavity tumors already reported in the species, such as peripheral odontogenic fibroma, mucoepidermoid carcinoma of the salivary gland, melanomas, hemangiosarcomas and fibrosarcomas.<sup>20,22-24</sup>

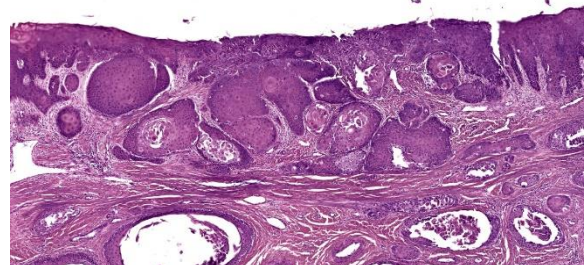


**Figure 1-3. Mandible, lion. Neoplastic squamous epithelium extends downward in irregular trabeculae and islands from the oral mucosa. (HE, 57X)**

**Contributing Institution:**

Federal Rural University of Pernambuco  
Laboratory of Animal Diagnosis  
Rua Dom Manoel de Medeiros  
Dois Irmaos, Recife, 52171-900  
Pernambuco, Brazil. www.ufrpe.br

**JPC Diagnosis:**

Mucosal surface (presumptive oral mucosa):  
Squamous cell carcinoma.

**JPC Comment:**

This week's moderator was Major Anna Travis, JPC Chief of Education Operations who selected an eclectic group of cases for conference participants to consider.

The contributor nicely summarizes oral SCC and oral pathology in non-domestic felids, to include a number of helpful references for those interested in reading further on this topic. Squamous cell carcinoma is the most common oral malignancy in all felids, including non-domestic ones.<sup>20</sup> Other notable oral predilections include FEPLOs in lions, oral papillomas in snow leopards, and eosinophilic inflammation in tigers.<sup>20</sup>

SCC remains a frequent WSC submission across species – the case discussion focused on associated general pathology features common across species, including keratinization. Basal cells exhibit basophilia in part due to large numbers of free ribosomes producing keratin filaments (protein; tonofilaments) that give strength to the epidermal layer. In the stratum spinosum, an even greater proportion of tonofilaments are bundled to form tonofibrils that interface with a greater number of desmosomes which further enhances tissue strength.<sup>25</sup> In the granular layer, keratohyalin granules containing profilaggrin serve to bind tonofibrils into larger macrofibrils. Squamous cells subsequently lose cellular organelles and nuclear contents as they transition to the stratum corneum.<sup>25</sup> As such, SCC represents

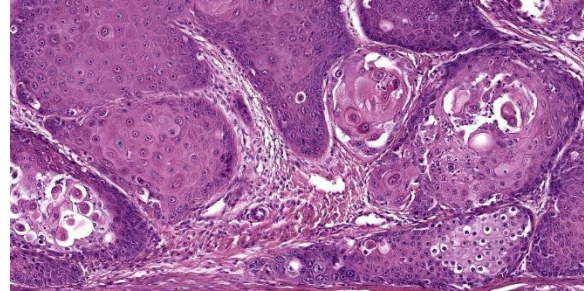


**Figure 1-4. Mandible, lion. High magnification of neoplastic squamous epithelium. Within the center of nests, neoplastic cells often become individualized. (HE, 57X)**

aberrancy of ordered keratinization as was evident in this case.

Conference participants discussed the exact location of this neoplasm as they lacked the terrific gross image for this case provided by the contributor. While the lack of adnexal units and presence of a non-keratinizing (lacking keratohyalin granules) epithelium were suggestive of the oral cavity, MAJ Travis reminded participants to also consider the pharynx, conjunctiva, esophagus, rectum, vulva, and even vagina as potential locations (although in felids, the oral mucosa is by far the most common location for this neoplasm).

**References:**

1. Murphy BG, Bell CM, Soukup JW. *Veterinary Oral and Maxillofacial Pathology*. 1st ed. Wiley-Blackwell; 2020:143.
2. Altamura G, Eleni C, Meoli R, et al. Tongue Squamous Cell Carcinoma in a European Lynx (*Lynx Lynx*): Papillomavirus Infection and Histologic Analysis. *Vet Sci*. 2018; 5(1):1.
3. Sladakovic I, Burnum A, Blas-Machado U, et al. Mandibular squamous cell carcinoma in a bobcat (*Lynx rufus*). *J Zoo Wildl Med*. 2016; 47(1): 370-373.
4. Yanai T, Noda A, Murata K, et al. Lingual squamous cell carcinoma in an ocelot (*Felis pardalis*). *Vet Rec*. 2003;

- 152(21):656-657.
5. Quintard B, Greunz EM, Lefaux B, et al. Squamous cell carcinoma in two snow leopards (*Uncia uncia*) with unusual auricular presentation. *J Zoo Wildl Med.* 2017; 48(2):578–580.
  6. Leme MCM, Martins AMCRPF, Bodini MES, et al. Carcinoma de células escamosas em uma jaguatirica (*Leopardus pardalis*). *Arq Inst Biol.* 2003; 70(2):217-219.
  7. Bose VSC, Nath I, Mohanty J, et al. Epidermoid carcinoma of the eyelid in a tiger (*Panthera tigris*). *Zoos' Print*, 2002; 17:965-966.
  8. Gupta A, Jadav K, Nigam P, et al. Eyelid neoplasm in a White Tiger (*Panthera tigris*) - a case report. *Vet Archiv.* 2013; 83(1):115-124.
  9. Oliveira AR, Carvalho T, Arenales A, et al. Mandibular squamous cell carcinoma in a captive Siberian tiger (*Panthera tigris altaica*). *Braz J Vet Pathol.* 2018; 11:97-101.
  10. Kedsangsakonwut S, Sanannu S, Rung-sipipat A, et al. Well-differentiated Squamous Cell Carcinoma in a Captive Clouded Leopard (*Neofelis nebulosa*). *Thai J Vet Med.* 2014; 44(1):153-157.
  11. Napier JE, Lund MS, Armstrong DL, et al. A retrospective study of morbidity and mortality in the North American amur leopard (*Panthera pardus orientalis*) population in zoologic institutions from 1992 to 2014. *J Zoo Wildl Med.* 2018; 49(1):70–78.
  12. Joslin JO, Garner M, Collins D, et al. Viral papilloma and squamous cell carcinomas in snow leopards (*Uncia uncia*). *American Association of Zoo Veterinarians and International Association for Aquatic Animal Medicine Joint Conference*, 2000: 155–158.
  13. Bertone ER, Snyder LA, Moore AS. Environmental and Lifestyle Risk Factors for Oral Squamous Cell Carcinoma in Domestic Cats. *J Vet Intern Med.* 2003; 17(4):557-562.
  14. Munday JS, Howe L, French A, et al. Detection of papillomaviral DNA sequences in a feline oral squamous cell carcinoma. *Res Vet Sci.* 2009; 86(2): 359–361.
  15. Sundberg JP, Montali RJ, Bush R, et al. Papillomavirus-associated focal oral hyperplasia in wild and captive Asian lions (*Panthera leo persica*). *J Zoo Wildl Med.* 1996; 27(1):61–70.
  16. Terio KA, McAloose D, Mitchell E. *Pathology of Wildlife and Zoo Animals.* 1st ed. Elsevier; 2018:263-285.
  17. Collados J, Garcia C, Soltero-Rivera M, et al. Dental Pathology of the Iberian Lynx (*Lynx pardinus*), Part II: Periodontal Disease, Tooth Resorption, and Oral Neoplasia. *J Vet Dent.* 2018; 35(3):209–216.
  18. Kapoor V, Antonelli T, Parkinson JA, et al. Oral health correlates of captivity. *Res Vet Sci.* 2016; 107:213-219.
  19. Castro MB, Barbeitas M, Borges T, et al. Fibromatous Epulis in a Captive Lion (*Panthera leo*). *Braz J Vet Pathol.* 2011; 4:150-152.
  20. Scott KL, Garner MM, Murphy BG, et al. Oral Lesions in Captive Nondomestic Felids With a Focus on Odontogenic Lesions. *Vet Pathol.* 2020; 57(6):880-884.
  21. Northrup NC, Selting KA, Rassnick KM, et al. Outcomes of cats with oral tumors treated with mandibulectomy: 42 cases. *J Am Anim Hosp Assoc.* 2006; 42(5):350-360.
  22. Junginger J, Hansmann F, Herder V, et al. Pathology in Captive Wild Felids at German Zoological Gardens. *PLoS One.* 2015; 10(6):e0130573.
  23. Kloft HM, Ramsay EC, Sula MM. Neoplasia in Captive *Panthera* Species. *J Comp Pathol.* 2019; 166:35-44.
  24. Steeil JC, Schumacher J, Baine K, et al. Diagnosis and treatment of a dermal malignant melanoma in an African lion

(Panthera leo). *J Zoo Wildl Med.* 2013; 44(3):721-727.

25. Welle MM, Linder KE. The Integument. In: Zachary JF, ed. *Pathologic Basis of Veterinary Disease.* 7th ed. St. Louis, MO: Elsevier; 2022:1095-1096.

## **CASE II:**

### **Signalment:**

Adult, female, Sprague-Dawley rat (*Rattus norvegicus*)

### **History:**

An adult, female, Sprague-Dawley rat, belonging to an intentional breeding colony was presented for diagnostic investigation of hind limb paresis. This animal had been fed Certified Rodent Diet 5002 (PMI Feeds, Inc) and given municipal water *ad libitum*, and only used for intravenous administration training without any active pharmaceutical ingredient. All procedures performed on the animal were in accordance with regulations and established guidelines reviewed and approved by an Institutional Animal Care and Use Committee.



**Figure 2-1. Lymph nodes, rat.** Cervical and mandibular lymph nodes are enlarged and greenish. (Photo courtesy of: Pfizer Drug Safety Research and Development, <https://www.pfizer.com/partners/research-and-development>).

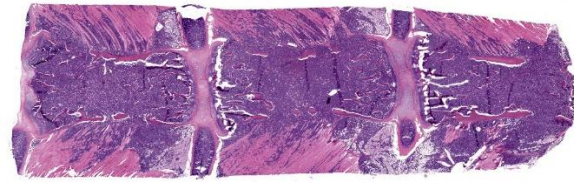


**Figure 2-2. Sternum, rat.** A section of sternum is submitted for examination. Neoplastic cells efface the marrow of the sternbrae and extend through the cortex into the adjacent skeletal muscle. (HE, 11X)

### **Gross Pathology:**

A gross examination revealed enlargement and greenish discoloration of multiple lymph nodes, including iliac, inguinal, mesenteric, popliteal, and mandibular lymph nodes. The spleen was also enlarged and the femoral bone marrow appeared green. A comprehensive set of tissues were collected in 10% neutral buffered formalin. All collected tissues were routinely processed and stained with hematoxylin and eosin (H&E) for light microscopic examination.

### **Microscopic Description:**

Sternum, bone marrow: Neoplastic cells had large, vesicular nuclei that varied in shape from round, segmented, lobulated, to ring shaped, and contained a small amount of slightly eosinophilic cytoplasm. They were noncohesive and arranged in diffuse sheets. There were approximately 5 mitotic figures per high power (400X magnification) field noted in the neoplastic cells in the bone marrow. Throughout the sheets of neoplastic cells in many of the affected tissues, there were small to moderate numbers of scattered large macrophages that contained phagocytized apoptotic cell debris.

Neoplastic cells completely replaced the normal hematopoietic elements in the medullary cavity of the sternum and had infiltrated into the surrounding bone, skeletal muscles, and joints.

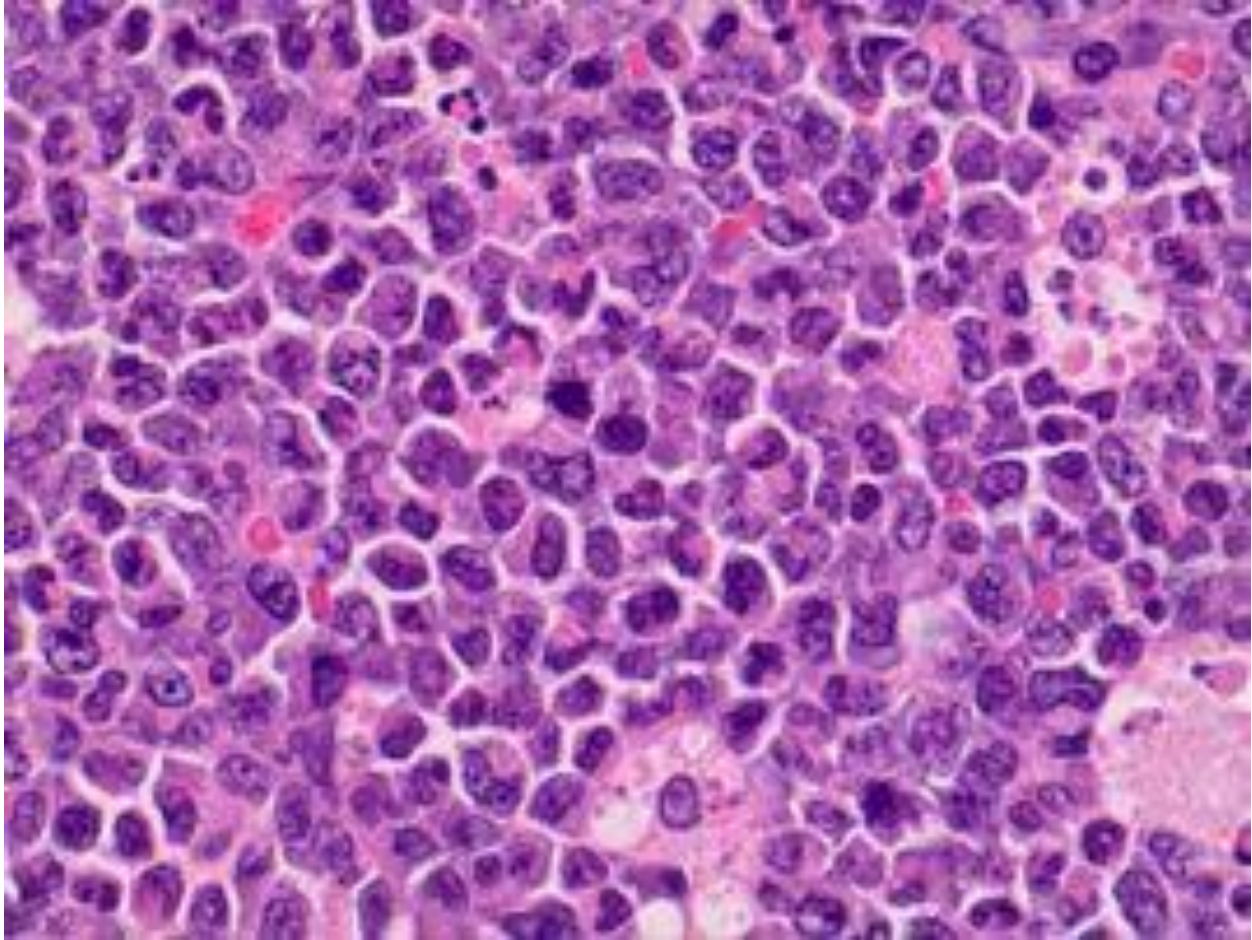


**Figure 2-3. Bone marrow, rat. Neoplastic cells have large, vesicular nuclei that varied in shape from round, segmented, lobulated, to ring shaped. Note there are scattered apoptotic figures. (HE, 400X) (Photo courtesy of: Pfizer Drug Safety Research and Development, <https://www.pfizer.com/partners/research-and-development>)**

Representative sections were selected for Iba-1 and MPO (myeloperoxidase) immunohistochemistry (IHC). Immunohistochemically, neoplastic cells within the bone marrow had strong cytoplasmic immunoreactivity for MPO, which is the hallmark of the myeloid lineage. Cellular debris-laden macrophages scattered throughout the sheets of neoplastic cells had strong membranous immunoreactivity for Iba-1, a macrophage marker.

**Contributor's Morphologic Diagnosis:**

Sternum/Bone marrow, myeloid leukemia in a Sprague-Dawley Rat

**Contributor's Comment:**

The current case was diagnosed as myeloid leukemia based on the characteristic cytological morphology and immunohistochemistry profile of the neoplastic cells. Various amounts of nuclear indentation noted among neoplastic cells was indicative of granulocytic differentiation and was suggestive of a more chronic leukemic process. Diffuse immunoreactivity of neoplastic cells for MPO

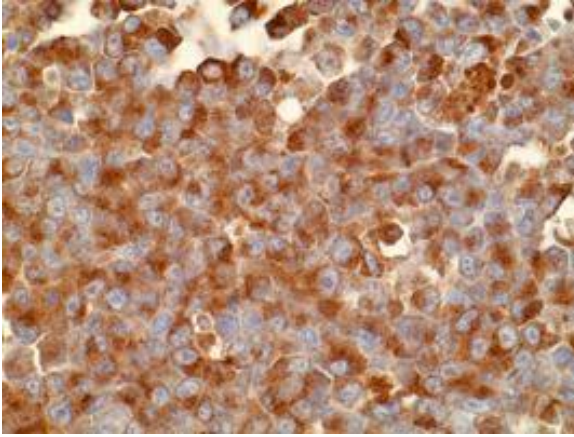


**Figure 2-4. Bone marrow, rat. Neoplastic cells have strong expression of cytoplasmic myeloperoxidase. (anti-MPO, 400X) (Photo courtesy of: Pfizer Drug Safety Research and Development, <https://www.pfizer.com/partners/research-and-development>)**

indicated that the cells stemmed from myeloid lineage because MPO is expressed by myeloid cells at all stages.

Massive inflammatory reactions to lesions in the skin or internal organs can stimulate compensatory myelopoiesis and result in remarkable extramedullary hematopoiesis and/or myeloid hyperplasia in the spleen and other organs as well as bone marrow, mimicking myeloid leukemia. The current case was differentiated from those compensatory reactions to inflammatory stimuli based on its invasive growth pattern, destruction of bone tissue associated with bone marrow proliferation, and the absence of inflammatory lesions.<sup>4,6</sup>

The macroscopic finding of green discoloration observed in the enlarged lymph nodes and bone marrow of the rat described in the current case report is associated with chloromas in humans, which has been described as a mass composed of immature granulocytic cells. This tumor occurs primarily in patients with myelogenous leukemia and typically has a green color caused by high levels of myeloperoxidase in those immature granulocytic cells.<sup>2</sup>

In the current case, the neoplasia was multicentric and with an invasive growth pattern. The presenting clinical finding of hind limb paresis was ascribed to extensive infiltration of neoplastic cells from the bone marrow through adjacent bones, joints, and skeletal muscles in the hind limb region. There was no evidence of tumor cell infiltration into the spinal cord or brain sections examined.

Hyaline droplets occurred in the renal proximal tubules in the current case. Hyaline droplets are known to accumulate in the identical segments of renal tubules in rats with a different neoplasm, histiocytic sarcoma. These droplets have been identified as lysozyme, which is a major secretory product of monocytes and macrophages.<sup>3</sup> It is important to note that IBA1 immunohistochemistry results demonstrated that apoptotic figures scattered throughout the sheets of neoplastic cells were cellular debris-laden macrophages. As with lysozyme in the case of histiocytic sarcoma, excessive production of this protein by activated macrophages is considered to be the likely cause of renal accumulation.

**Contributing Institution:**

Pfizer Drug Safety Research and Development  
455 Eastern Point Rd.,  
Groton, CT 06340  
<https://www.pfizer.com/partners/research-and-development>

**JPC Diagnosis:**

Bone marrow and skeletal muscle: Myeloid leukemia.

**JPC Comment:**

We agree with the contributor that the tissue submitted represents a hematopoietic neoplasm for the histologic features they so nicely capture in their discussion. Conference participants honed in on infiltration of the

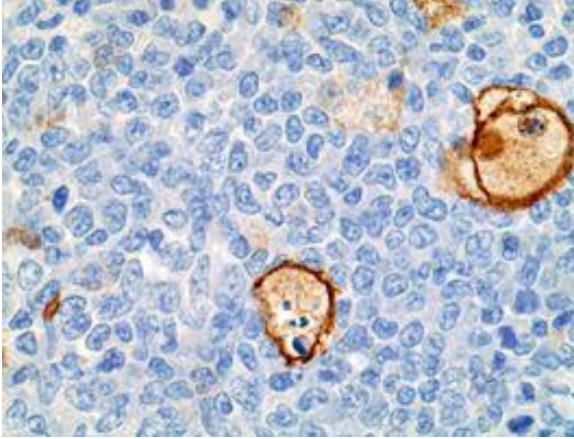


**Figure 2-5. Bone marrow, rat. Scattered large macrophages that contain phagocytized apoptotic cell debris (apoptotic figures) have strong membranous expression of Iba-1 (anti-IBA1, 400X) (Photo courtesy of: Pfizer Drug Safety Research and Development, <https://www.pfizer.com/partners/research-and-development>)**

surrounding adipose tissue and muscle by neoplastic cells as well as the effacement of the marrow cavity and loss of trabecular and cortical bone as major features of this case.

We performed IHCs for IBA1, myeloperoxidase, lysozyme, CD3, CD33, CD34, CD56, CD117, PAX5, as well as an EBER ISH. We confirmed the background of tumor-associated macrophages with IBA1 (while also ruling out histiocytic sarcoma), though our results for MPO, lysozyme, CD33, and CD34 were equivocal and we could not reproduce the contributor's IHC result. Curiously, we did note moderate immunoreactivity of neoplastic cells for CD3 and CD56 which suggests a potential (although we feel unlikely) potential T-lymphocyte origin for these cells, though our lab is not optimized for rodent IHCs. As such, we rendered a H&E diagnosis for the case. ISH and other IHCs for this case were unremarkable.

We previously covered hyaline droplets in rodents in a recent (WSC 24-25, Conference 6, Case 1) which featured a histiocytic

sarcoma within the kidney itself. We also considered myeloid leukemia in that case – incidentally, the morphology of neoplastic cells is very similar. Ruleouts for hyaline droplets include histiocytic sarcoma,<sup>3</sup> lymphoma,<sup>1</sup> chronic progressive nephropathy, and alpha-2u globulin nephropathy.<sup>5</sup>

#### **References:**

1. Decker JH, Dochterman LW, Niquette AL, et al. Association of Renal Tubular Hyaline Droplets with Lymphoma in CD-1 Mice. *Toxicol Pathol.* 2012; 40: 651-655.
2. Ginsberg LE, Leeds NE. Neuroradiology of leukemia. *AJR.* 1995;165:525-534.
3. Hard GC, Snowden RT. Hyaline droplet accumulation in rodent kidney proximal tubules: An association with histiocytic sarcoma. *Toxicol Pathol.* 1991;19:88-97.
4. Long RE, Knutsen G, Robinson M. Myeloid hyperplasia in the SENCAR mouse: Differentiation from granulocytic leukemia. *Environ Health Persp.* 1986;68:117-123.
5. Swenberg JA, Short B, Borghoff S, Strasser J, Charbonneau M. The comparative pathobiology of alpha 2u-globulin nephropathy. *Toxicol Appl Pharmacol.* 1989 Jan;97(1):35-46.
6. Ward JM, Rehg JE, Morse HC. Differentiation of rodent immune and hematopoietic system reactive lesions from neoplasia. *Toxicol Pathol.* 2012;40:425-434.

#### **CASE III:**

##### **Signalment:**

Juvenile, female, giant Pacific octopus (*Enteroctopus dofleini*)

##### **History:**

This giant Pacific octopus arrived at the submitting zoo after an extended period at an outgoing airport. During the first week at the

zoo, the animal was eating well but was staying at the bottom of the enclosure. Shortly thereafter, the octopus stopped eating and was found to have several injuries consistent with self-mutilation and damage by the co-habitant anemones. Water quality was within normal limits. The octopus was found deceased a few days later.

### **Gross Pathology:**

Macroscopic lesions included skin erosions and ulcerations and distal limb amputations. The digestive gland was uniformly soft, tan-pink, and bulging on cut section. There were no significant macroscopic lesions of the renal appendages.

### **Laboratory Results:**

Aerobic culture of the digestive gland yielded *Carnobacterium* sp. (1+ mixed) and *Vibrio* sp. (4+ predominant).

### **Microscopic Description:**

Renal appendage: The renal appendage is composed of folds and tubules lined by simple columnar epithelium supported by a fibrovascular stroma and separated by venous sinuses. The epithelial cells are large, with basal nuclei, mild apical vacuolation, and a brush border. Anisocytosis and anisokaryosis of the renal epithelial cells is moderate to marked. Copious globular, eosinophilic material is present within tubule lumina, and homogeneous, eosinophilic secretory product multifocally fills sinus lumina. Along the epithelial surfaces, there are innumerable cross-sectional and tangential profiles of multicellular, vermiform organisms at various stages of maturation, with no apparent associated inflammatory reaction. The organisms measure approximately 25 to 100 micrometers in diameter and consist of a central axial cell enveloped completely by a layer of ciliated peripheral cells. Several large peripheral cells with short or inapparent cilia comprise the anterior ends of the organisms (interpreted as

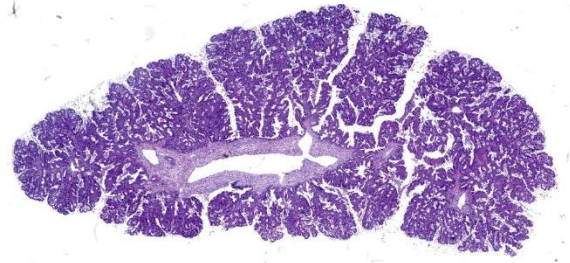


**Figure 3-1. Renal appendage, octopus. One section of renal appendage is submitted for examination. (HE, 7X)**

the calotte), which commonly abut the renal epithelial cells and obscure the brush border. At these sites, the epithelial cells are variably attenuated. Within the axial cell cytoplasm in a majority of the organisms, there are one or more developing embryos and single cells (agametes or fertilized eggs). The developing embryos are multicellular, often organized into an elongate structure or forming a round to oval cluster of cells (vermiform and infusoriform embryos).

### **Contributor's Morphologic Diagnosis:**

Renal appendage: intraluminal dicyemid organisms, widespread, marked, chronic

### **Contributor's Comment:**

The renal organs of octopuses consist of folded tissue that protrudes into the renal sac. The degree of tissue folding generally increases with the size of the organism and increases excretory capacity.<sup>10</sup> The folds form tubules lined by a simple columnar epithelium and separated by sinuses that originate from the vena cava. Within the tubule and renal sac lumina, one may find a variety of worm-like dicyemid organisms that are often attached to the renal epithelium without eliciting an inflammatory response.<sup>1,3</sup>

Dicyemids (phylum Dicyemida) are mesozoans found within the renal organs of many cephalopod species, and were an incidental finding in this giant Pacific octopus (Enter

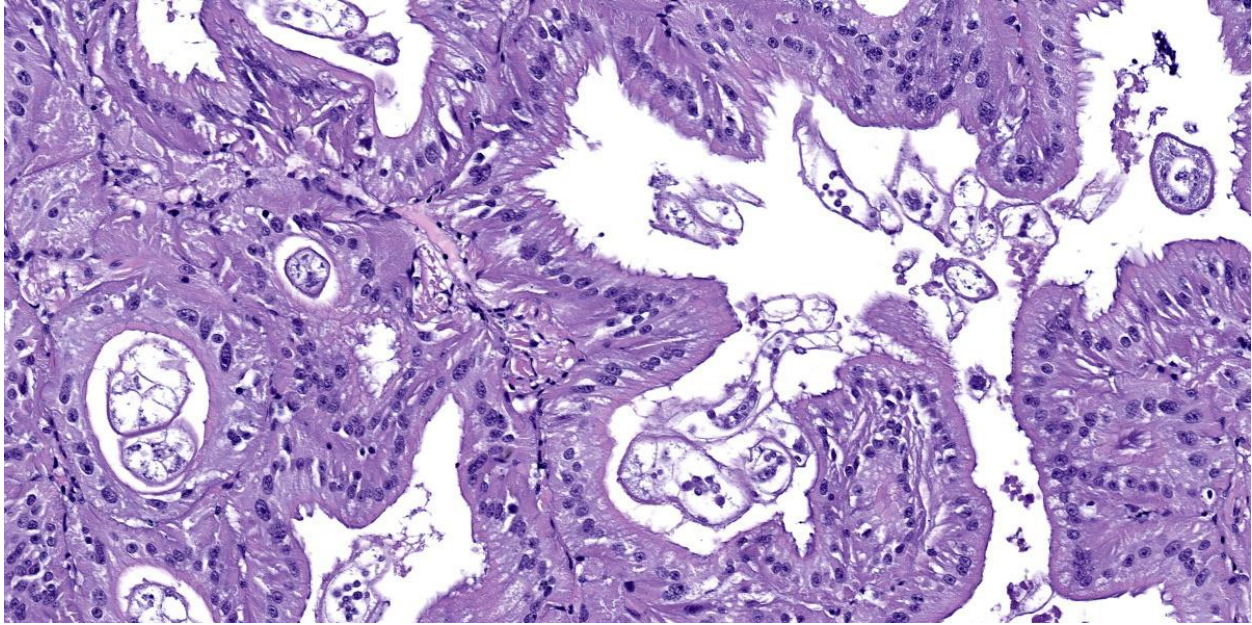


**Figure 3-2. Renal appendage, octopus. Within the sinus lumina, there are numerous cross- and tangential sections of multicellular, vermiform organisms at various stages of maturation, with no apparent associated inflammatory reaction. The organisms measure approximately 25 to 100 micrometers in diameter and consist of a central axial cell enveloped completely by a layer of ciliated peripheral cells. (HE, 202X)**

octopus *dofleini*). Dicyemids have been variably described as endosymbionts and as endoparasites, as they attach to the renal epithelium of the host, absorb nutrients from the urine through their peripheral cells, and can be present in large numbers. Regardless, they have not been shown to damage the renal organs or be detrimental to the host.<sup>1</sup> Their postulated benefits include acidification of the urine to aid excretion of ammonia and maintenance of urine flow by their ciliary movements.<sup>1,10,14</sup>

There are 149 documented dicyemid species to date, all of which exhibit a remarkably simple body plan that left many questions about their evolutionary origins.<sup>15</sup> They were initially classified as mesozoa for presumptively representing an intermediate between protozoa and metazoa. While the phylogenetic particulars of these organisms are arguably uncertain, current evidence indicates

they arose from metazoan ancestors as a result of evolutionary simplification with genome reduction.<sup>4,14</sup>

The dicyemid life cycle consists of vermiform and infusoriform stages. Mature dicyemids are vermiform and exist within the renal organ as a nematogen, a primary rhombogen, or a secondary rhombogen.<sup>11</sup> These adults possess a central axial cell with intracytoplasmic agametes that is fully surrounded by 8 to 30 ciliated peripheral cells. Four to ten peripheral cells at the anterior aspect of the organism form a calotte, which interacts with the host renal epithelium.<sup>15</sup>

Nematogens reproduce asexually. An agamete within the axial cell cytoplasm develops into a vermiform embryo, which then exits the adult through a gap between peripheral cell membranes or by penetrating a peripheral cell.<sup>12,13</sup> The vermiform larva matures into either another nematogen or a primary

rhombogen and remains within the host. In contrast, primary rhombogens and secondary rhombogens, which transition from nematogens rather than mature from vermiform larvae, reproduce sexually. An agamete within the axial cell develops into an infusorigen, a hermaphroditic gonad that gives rise to oocytes and spermatocytes. Fertilization results in development of infusoriform embryos, which escape the parent organism in a manner similar to vermiform embryos.<sup>10</sup> While the vermiform stages are confined to the renal organs, infusoriform larvae can exit the renal organ, escape the original host, and eventually infect a new host by an unknown mechanism.<sup>12</sup> Many dicyemid species exhibit high host specificity, and two or three species are commonly found within a single cephalopod host.<sup>15</sup>

Vermiform larvae exhibit a body plan similar to the adults. Contrarily, infusoriform larvae are composed of a higher number and greater variety of cells, resulting in diverse body organizations of at least 14 different cell types.<sup>8</sup> The number of peripheral cells in the adults, the shape and organization of the calotte, the number of total and peripheral cells in vermiform embryos, and the number and organization of cells in infusoriform embryos are species-specific.<sup>7-9,12</sup> Distinguishing between dicyemid species, rhombogen and nematogen forms, and vermiform and infusoriform embryos in routine histologic sections seems quite challenging, and may be best attempted using tissue smears and particular fixation and storage techniques.

**Contributing Institution:**

University of Minnesota Veterinary Diagnostic Laboratory  
<https://vdl.umn.edu/>

**JPC Diagnosis:**

Renal appendage: Nephritis, hemocytic, acute, multifocal, mild with vasculitis.

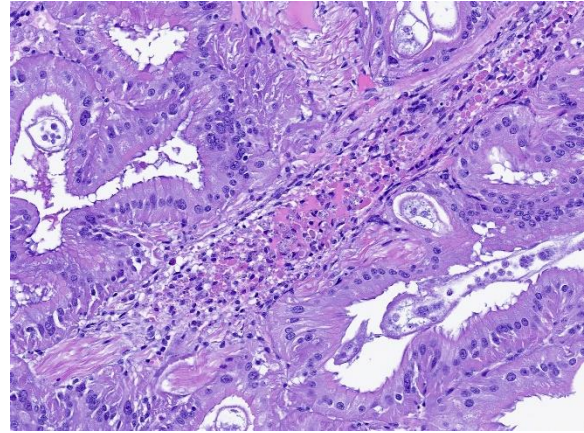


**Figure 3-3. Renal appendage, octopus. There is hemocytic vasculitis within the hemolymphatic vessels. (HE, 200X)**

**JPC Comment:**

We thank the contributor for sharing this unique tissue with us in conference. Invertebrate pathology was a recent focus of *Veterinary Pathology*<sup>2</sup> and the present section is an opportunity to build familiarity both with invertebrate anatomy and a common background commensal organism in octopuses. Additionally, tissue (digestive gland) from this case was also presented at the 2024 Davis-Thompson Foundation Invertebrate Histology Seminar – Dr. Elise Ladouceur was one of the moderators and weighed in similarly on this case.

The contributor provides a terrific summary of dicyemid background biology and intersection with normal octopus physiology. Although not a lesion *per se*, recognizing these as normal organisms and avoid diagnosing pathologic parasitism merits discussion among a wider audience. Conference participants hotly debated how to best capture the role of dicyemids in this case. As we typically do not create morphologic diagnoses for non-lesions, we were rescued in this case by a less prominent pathologic finding. Nonetheless, we concur with the presence of renal dicyemids, a routine finding in octopuses that should not be interpreted as a lesion. Dr. Ladouceur also noted that reduced numbers or

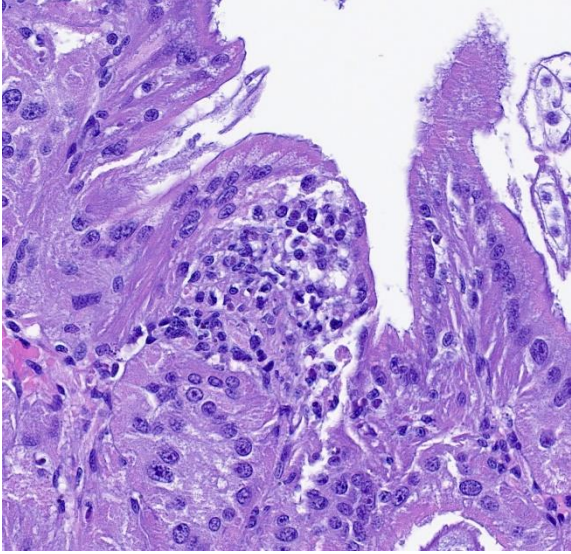


**Figure 3-4. Renal appendage, octopus. There are scattered foci of hemocytic inflammation within the parenchyma of the renal appendage. (HE, 400X)**

absence of renal dicyemids may represent loss of fitness, though this remains speculative.

Although somewhat subtle, there was also evidence of multifocal inflammation in the renal appendage. This was likely secondary to bacterial sepsis, consistent with the contributor's aerobic culture of the digestive gland which yielded both *Carnobacterium* and *Vibrio* species. Hemocytic inflammation effaced the walls of hemolymphatic vessels and was associated with karyorrhexis, consistent with vasculitis. Although not part of the reviewed tissues, follow up with the contributor confirmed that this animal had severe interstitial inflammation in the digestive gland centered on gram negative, curved bacilli which was consistent with *Vibrio* spp. infection. *Vibrio* spp. have been frequently isolated from skin lesions and/or organs or fluid (hemolymph) of larval, juvenile, and adult octopuses.<sup>5,6</sup> Additionally, other bacteria associated with mortality and sepsis in octopuses include *Pseudomonas* spp. and *Aeromonas* spp.,<sup>5,6</sup> though discerning the ability

of these bacteria to cause primary disease, especially in mixed bacterial culture with *Vibrio*, remains uncertain. Preventative health measures such as tank cleaning and water quality management remain important considerations for captive cephalopod husbandry.<sup>6</sup>

#### References:

1. Anadón R. Functional Histology: The Tissues of Common Coleoid Cephalopods. In: Gestal C, Pascual S, Guerra Á, Fiorito G, Vieites JM, eds. *Handbook of Pathogens and Diseases in Cephalopods*. Springer Open; 2019.
2. Dennis MM, LaDouceur EEB. Special focus issue on invertebrate pathology: A growing discipline requiring veterinary diagnosticians. *Veterinary Pathology*. 2023;60(5):501-502.
3. Dill-Okubo JA, Berzins IK, LaDouceur EEB, Camus AC. Mollusca: Cephalopoda. In: LaDouceur EEB, ed. *Invertebrate Histology*. John Wiley & Sons, Inc.; 2021.
4. Drábková M, et al. Different phylogenomic methods support monophyly of enigmatic 'Mesozoa' (Dicyemida + Orthonectida, Lophotrochozoa). *Proc R Soc B*. 2022;289(1978):20220683.
5. Farto R, Armada SP, Montes M, Guisande JA, Pérez MJ, Nieto TP. *Vibrio lentus* associated with diseased wild octopus (*Octopus vulgaris*). *J Invertebr Pathol*. 2003 Jun;83(2):149-56.
6. Farto R, Fichi G, Gestal C, Pascual S, Nieto TP. Bacteria-Affecting Cephalopods. In: Gestal C, Pascual S, Guerra Á, Fiorito G, Vieites J, eds. *Handbook of Pathogens and Diseases in Cephalopods*. Springer, Cham. 2019.

[https://doi.org/10.1007/978-3-030-11330-8\\_8](https://doi.org/10.1007/978-3-030-11330-8_8)

7. Furuya H, Hochberg FG, Tsuneki K. Calotte morphology in the phylum Dicyemida: niche separation and convergence. *J Zool.* 2003;259:361-373.
8. Furuya H, Hochberg FG, Tsuneki K. Cell Number and Cellular Composition in Infusoriform Larvae of Dicyemid Mesozoans (Phylum Dicyemida). *Zool Sci.* 2004;21:877-889.
9. Furuya H, Hochberg FG, Tsuneki K. Cell number and cellular composition in vermiform larvae of dicyemid mesozoans. *J Zool.* 2007;272:284-298.
10. Furuya H, Ota M, Kimura R, Tsuneki K. Renal Organs of Cephalopods: A Habitat for Dicyemids and Chromidinids. *J Morphol.* 2004;262:629-643.
11. Furuya H. Progenesis in dicyemids. *Invertebr Biol.* 2024;142:e12419.
12. Furuya H, Tsuneki K. Biology of Dicyemid Mesozoans. *Zool Sci.* 2003;20:519-532.
13. Hisayama N, Furuya H. Escape Processes in Embryos of Dicyemids (Phylum Dicyemida). *J Parasitol.* 2023;109(5):496-505.
14. Lu TM, Kanda M, Furuya H, Satoh N. Dicyemid Mesozoans: A Unique Parasitic Lifestyle and a Reduced Genome. *Genome Biol Evol.* 2019;11(8):2232-2243.
15. Nakajima H, Fukui A, Suzuki K, Tirta RYK, Furuya H. Host Switching in Dicyemids (Phylum Dicyemida). *J Parasitol.* 2024;110(2):159-169.

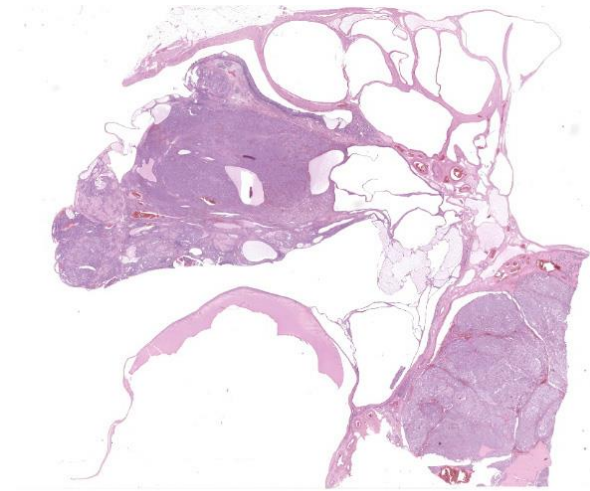


**Figure 4-1. Ovary, dog. One section of ovary is submitted for examination. At subgross magnification, normal ovarian architecture is lost. There are numerous cysts measuring up to 5mm in diameter scattered throughout the section, and at least two neoplasms are visible (at upper left and lower right). (HE, 5X)**

#### **CASE IV:**

##### **Signalment:**

12 years old and 3 months, female (neutered), Golden retriever, *Canis lupus familiaris*, canine

##### **History:**

The animal was surgically treated with ovari-hysterectomy due to pyometra. Both ovaries and uterus were formalin-fixed and submitted for histopathological examination.

##### **Gross Pathology:**

Macroscopically, right and left ovary appeared to be increased in size. Right ovary was 3x5 cm and left ovary was 8x6 cm. In addition, both uterus and ovaries had multiple nodules and cysts, the latter containing macroscopically transparent fluid.

##### **Laboratory Results:**

Below is a table reporting the results of the immunohistochemical analysis (Tab. 1).

**Table 1.** Right ovary: results of immunohistochemical analysis performed by our laboratory in comparison with the positivities reported in literature for the three tumors. The positivity was cytoplasmic and diffuse in the whole tumoral population if not otherwise specified into the table.

Tested antigen	Present study			Literature		
	Epithelial tumor	Granulosa cell tumor	Dysgerminoma	Epithelial tumor	Granulosa cell tumor	Dysgerminoma
panCK	++	+	-	P <sup>1,2,5,8,10,11,12</sup>	P/N <sup>1,2,5,8,10,11,12</sup>	N <sup>1,2,5,8,10,11,12</sup>
Vimentin	++	++	++	P/N <sup>1,2,3,5,8,10,11,12</sup>	P <sup>1,2,3,5,8,10,11,12</sup>	P <sup>1,2,3,5,8,10,11,12</sup>
HER-2	+/- <sup>§</sup>	+/- <sup>§</sup>	-	N <sup>7</sup>	P/N <sup>7</sup>	N <sup>7</sup>
c-kit	-	-	-	P/N <sup>11,17</sup>	N <sup>11,17</sup>	P/N <sup>11,17</sup>
SMA	-	-	-	P/N <sup>3</sup>	P/N <sup>3</sup>	ND <sup>3</sup>
Desmin	++/+ <sup>*</sup> (multifocal)	-	+/- <sup>**</sup> (multifocal)	P/N <sup>2,3</sup>	P/N <sup>2,3</sup>	P/N <sup>2,3</sup>

++ = strong positivity; + = moderate positivity; +/- = weak positivity; - = no positivity

P = positive; N = negative; P/N: some positive and some negative cases; ND: not determined

<sup>§</sup>HER-2 positivity was considered +/- since complete membrane staining was not observed in >10% of cells.

\*Some areas were strong and some moderate in positivity. Some areas were negative.

\*\*Perinuclear spotted positivity

## Microscopic Description:

### Right ovary:

Continuous with the ovarian surface epithelium, occupying 20% of the section and replacing the normal ovarian tissue, there is a moderately cellular, not well demarcated, non-encapsulated and non-infiltrative neoplastic population. The neoplasm is characterized by endophytic and esophytic tubular and tubulo-papillary structures, associated with moderate to abundant ovarian fibrovascular stroma. Tubules are occasionally ectatic and contain a moderate amount of often homogeneously eosinophilic amorphous material.

Neoplastic cells are cuboidal to columnar with indistinct cell borders, scant eosinophilic cytoplasm and round to oval (10 um) eccentrically located nuclei with finely stippled chromatin and mainly 1 distinct nucleolus. Anisocytosis and anisokaryosis are mild. Mitoses are rare (< 1 per hpf).

Close to this neoplasm, multifocally colliding, there is a second densely cellular, well-

demarcated, non-encapsulated and infiltrative neoplasm occupying 40% of the section. The neoplasm is characterized by sheets of cells admixed with a very fine and scant fibrovascular stroma.

Neoplastic cells are irregularly round with distinct cell borders (up to 20 um), moderate to abundant occasionally granular slightly eosinophilic cytoplasm, occasionally showing single to multiple large empty well-defined vacuoles.

The nucleus is round to oval, rarely megalic (macrokaryosis) with finely stippled chromatin and 1 distinct nucleolus. Anisocytosis and anisokaryosis are moderate with occasional bi and multinucleation. Mitoses are on average 2-4 per high power field.

Multifocal mild hemorrhages are evident, as well as disseminated single cell necrosis/apoptosis. Entrapped in the neoplasm, there are occasional ectatic and cystic tubular structures lined by a cuboidal to flattened epithelium.

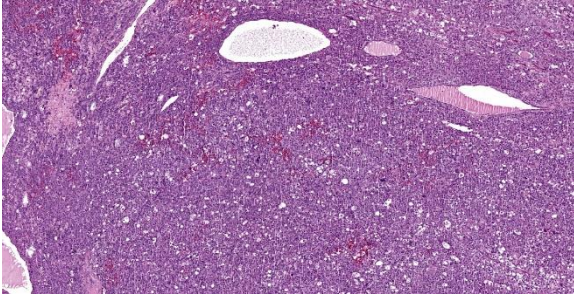


**Figure 4-2. Ovary, dog. One neoplasm is composed of germ cells arranged in sheets (dysgerminoma) (HE, 60X)**

At the periphery of both the neoplasms and close or involving the rete ovarii, multiple variably-sized ovarian and para-ovarian epithelial and vascular cystic spaces occasionally containing a variable amount of slightly eosinophilic amorphous material are also observed.

Close to the cystic portion, occupying 20% of the section there is a densely cellular, well demarcated, non-encapsulated and non-infiltrative neoplasm. The cells form mainly nest and tubular structures, the latter mainly with small lumens (microfollicular), separated by variably sized bands of scant fibrovascular stroma. Neoplastic cells are irregularly oval to elongated with indistinct cell borders, moderate eosinophilic fibrillar to vacuolized cytoplasm with small (5-7  $\mu$ m) hyperchromatic round to oval nuclei. Anisocytosis and anisocytosis are mild. Neoplastic cells focally surround microcavities containing intensely eosinophilic amorphous material (Call-Exner bodies). Mitoses are rare (<1 per hpf). Multifocal haemorrhagic lacunae are also present.

**Contributor's Morphologic Diagnosis:**

Right Ovary: papillary adenoma, dysgerminoma and granulosa cell tumor associated with multiple ovarian and para-ovarian cysts.

Left ovary (not submitted): dysgerminoma

Uterus (not submitted): cystic endometrial hyperplasia and purulent endometritis

**Contributor's Comment:**

This was a very unusual case of three different tumors in the same ovary of an adult female dog.

Ovarian tumors are described as a frequent condition in female dogs, but epidemiological data are incomplete. They occur more often in older animals, and usually are noted due to behavioral changes. Additionally, lactation and vaginal discharge can also be present. They also can be associated with ovarian cysts and with uterine lesions such as cystic endometrial hyperplasia and pyometra.<sup>9,16</sup>

Typically, ovarian tumors grow as single subtype either monolaterally, or less often, bilaterally with the latter being mainly represented by sex cord stromal tumors.<sup>9</sup> Only rare cases of simultaneous neoplastic lesions of different cell of origin have been described in ovaries. To our knowledge, there is only one case report of a concomitant teratoma and granulosa cell tumor growing distinctively into the two ovaries of an English Bulldog.<sup>8</sup>

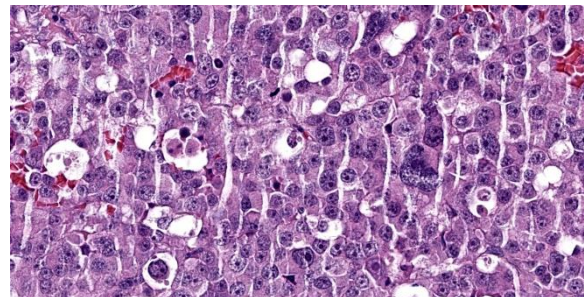


**Figure 4-3. Ovary, dog. Neoplastic germ cells demonstrate moderately pleomorphic nucleoli. (HE, 585X)**

**Table 2.** The expression of specific markers in normal human and canine epithelial, granulosa, and germ cells according to the literature.<sup>1-3,5-7,10-12,17</sup>

	Epithelial cells	Granulosa cells	Germ cells
<b>Human</b>	CKAE1/AE3, CK7 CK8 CK10 CK18 HBME-1 MUC1 VIM 17b-hydroxysteroid dehydrogenase Integrin N-cadherin	CKAE1/AE3 INH- $\alpha$ N-cadherin VIM	OCT3/4 SALL4 PLAP Protein VASA
<b>Dog</b>	CKAE1/AE3 CK7 HBME-1	CK AE1/AE3 INH- $\alpha$ VIM	OCT 3/4 SALL4 PLAP

CK = cytokeratin; HBME-1 = Hecto Battifora mesothelial epitope-1; MUC1 = cell surface associated mucin1; VIM = vimentin; INH-  $\alpha$  = inhibin- $\alpha$ ; OCT = Octamer-binding transcription factor; SALL4 = Sal-like protein 4; PLAP = Placental alkaline phosphatase.

Papillary adenoma is a benign tumor of the surface epithelium mainly described in the bitch. Usually at the cut surface there are multiple small cysts which are a feature of this type of tumor.<sup>5</sup> The neoplasm can be smooth and nodular, or when arising on the surface, give the ovary a cauliflower-like appearance. There is scant connective stroma and the papillary projections are lined by small cuboidal to cylindrical cells that may have cilia. Mitotic figures are rare.<sup>12</sup> Papillary adenocarcinoma is the malignant counterpart of benign papillary adenomas.<sup>5</sup> Size is an important criterion of malignancy. Tumors that extend through the opening of the ovarian bursa are likely to be malignant and spread by implantation to the peritoneal surface. The surface of an adenocarcinoma tends to be shaggy, and it is the fronds that break off and give rise to metastatic implantations. This tumor is similar in origin and appearance to its benign counterpart, and distinguishing between them can be difficult. Additional criteria for malignancy are increased mitotic activity, invasion into the

ovarian stroma, and extension into the ovarian bursa.<sup>12</sup> Based on features in this case, we favored a papillary adenoma.

Dysgerminoma is a tumor that develops from germ cells before differentiation. It has been recognized most often in the bitch, but is much less common in female dogs than the male testicular counterpart (i.e. seminoma). Dysgerminomas are malignant and may metastasize or spread locally, but early spread is not common. Histologically, there are no defined criteria to predict tendency to metastasize.<sup>12</sup> Dysgerminomas are composed of a uniform population of large round cells with clear or light-staining amphophilic cytoplasm. The nuclei are centrally located and contain abundant granular chromatin and either one or two prominent nucleoli. Mitotic figures are often numerous, and incomplete division of tumor cells may result in multinucleated giant cells. Individual tumor cells may undergo necrosis, leaving a distinctive clear space. The stroma is

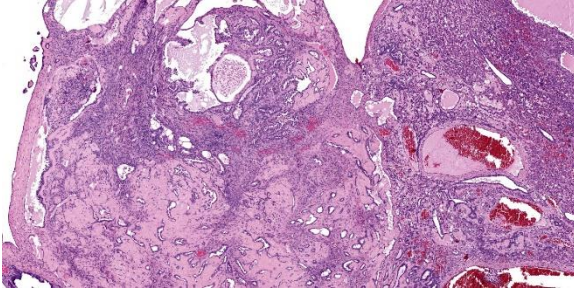


**Figure 4-4. Ovary, dog. Adjacent to the dysgerminoma, there is a papillary adenoma with hyalinized stroma. (HE, 53X)**

usually light and may be infiltrated with lymphocytes.<sup>12</sup>

Granulosa cell tumors are composed primarily of cells that resemble the granulosa cells of the ovarian follicle. They can develop from ovarian remnants and be either benign or malignant. The tumor often contains cells of the theca interna and fibroblasts. In the bitch, they are slightly less common than epithelial tumors of the ovary.<sup>12</sup> Steroidogenesis may be associated with granulosa cell tumors. Either estrogens or androgens can be produced, though not all granulosa cell tumors are hormonally active. Inhibin is regularly produced by granulosa cell tumors in the mare and is thought to be the cause of atrophy of the contralateral ovary.<sup>12</sup> Only rarely do granulosa cell tumors metastasize in cows or bitches, and such reports are even rarer in mares.<sup>12</sup> Neoplastic granulosa cells have spherical-to-oval, hyperchromatic nuclei, distinct nucleoli, and scant eosinophilic cytoplasm. The common patterns are follicular (microfollicular and macrofollicular), insular, trabecular, and diffuse. Often a combination of patterns exists in a single tumor. Call-Exner bodies, which are distinctive microcavities that contain watery or hyaline eosinophilic material and occasionally pyknotic nuclei are surrounded by granulosa cells in a rosette arrangement. These are seen most often in the microfollicular pattern. Some granulosa cell tumors, particularly those in the bitch, develop a tubular pattern similar to that of the Sertoli cell tumor of the testis,

and like Sertoli cell tumors some of these granulosa cell tumors induce a dense fibrous stroma. Theca cells may also be present in granulosa cell tumors. Either or both cell types may be luteinized.<sup>12</sup>

Expression markers of different normal ovarian cell type (Table 2) can be helpful to characterize tumors of different origin particularly when less differentiated as also reported in Table 1. The tumors reported in this case presented a IHC phenotype resembling what reported into the literature for the studied markers (Table 1).

In addition to the markers performed by our laboratory, CK7, PLAP and inhibin could also be performed to further confirm the tissue origin of the identified neoplasms.<sup>1,2,5,6,10,11,12</sup>

#### **Contributing Institution:**

Department of Comparative Biomedicine and Food Science (Università of Padua)

Viale dell'Università, 16 (35020), Legnaro (PD), Italy

<https://www.bca.unipd.it/>

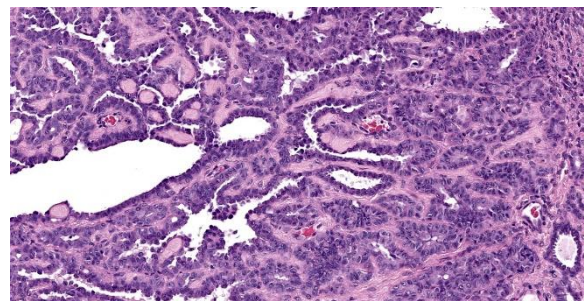


**Figure 4-5. Ovary, dog. Within the adenoma, epithelial cells are cuboidal, bland, and demonstrate no definitive evidence of infiltrative growth or cellular features of malignancy. (HE, 263X)**

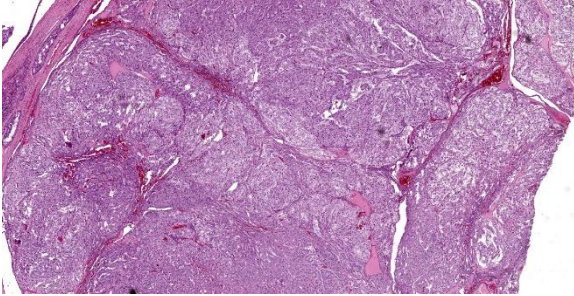


**Figure 4-6. Ovary, dog. A third neoplasm featuring cuboidal to columnar cells in tubules is present (granulosa cell tumor). (HE, 55X)**

**JPC Diagnosis:**

1. Ovary: Dysgerminoma.
2. Ovary: Papillary adenoma.
3. Ovary: Granulosa cell tumor.
4. Ovary: Cysts, multiple.

**JPC Comment:**

The final case of this conference features four separate entities to describe. Conference participants noted one or more neoplasms and cysts, though only a select few were tenacious enough to identify all 3 neoplastic cell populations. This is a unique slide that is a microcosm of ovarian neoplasia – it is a fine companion to the analogous testicular tumor case we reviewed in WSC 24-25 Conference 10 (Case 2 – also from a dog).

We agree with the contributor that multiple different ovarian neoplasms is not a common finding in the dog. Ovarian neoplasia itself is relatively rare in dogs, representing approximately 1-2% of all neoplasms.<sup>14,15</sup> Arriving at 3 separate neoplasms in a single ovary likely represents the confluence of multiple rare outcomes. That the contralateral ovary in this case (not included with this slide) also had a dysgerminoma could reflect either metastasis or a separate neoplasm arising spontaneously – the submission materials leave this aspect of the case open.

Identification of a granulosa cell tumor was straightforward in this case with recognition of Call-Exner bodies and fibrous tissue septa being helpful correlates. The intersection of the dysgerminoma and the adenoma is intriguing, but the two neoplasms are easily distinguished from each other. We considered the possibility of a ovarian carcinoma in this case, however, definitive areas of stromal invasion are not evident in these sections.

Lastly, we agreed with the contributor that there are multiple cysts present in this case, though we did not attempt to further classify each one, especially in light of the three distinct neoplasms in the surrounding tissue. Cystic structures arising from the ovary include cysts of the rete ovarii, subsurface epithelial structures, and follicle. Paraovarian cysts are located in tissue adjacent to the ovary and include remnants of the mesonephric duct, paramesonephric duct, and mesonephric tubule.<sup>13</sup> Features such as the presence of ciliated epithelium, smooth muscle in the cyst wall, and a basement membrane can be used to distinguish these diagnoses.<sup>13</sup> Location (if known) is also helpful discriminator.

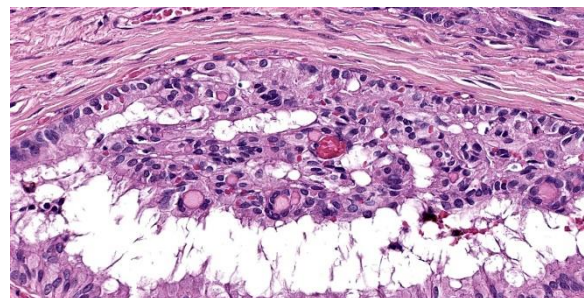


**Figure 4-7. Ovary, dog. Granulosa cells are present within tubules. They often palisade along basement membranes, and in some areas, surround hyaline eosinophilic material (Call-Exner bodies). (HE, 385X)**

## References:

1. Auersperg N, Wong AST, Choi K-C, Kang SK, Leung PCK. Ovarian Surface Epithelium: Biology, Endocrinology, and Pathology. 2001;22(2).
2. Akihara Y, Shimoyama Y, Kawasako K, et al. Immunohistochemical Evaluation of Canine Ovarian Tumors. *J Vet Med Sci.* 2007;69(7):703–708.
3. Czernobilsky B, Shezen E, Lifschitz-Mercer B, et al. Alpha smooth muscle actin (alpha-SM actin) in normal human ovaries, in ovarian stromal hyperplasia and in ovarian neoplasms. *Virchows Arch B Cell Pathol Incl Mol Pathol.* 1989;57(1):55-61.
4. Dolenšek T, Knific T, Ramírez GA, Erles K, Mallon HE, Priestnall SL, Suárez-Bonnet A. Canine ovarian epithelial tumours: histopathological and immunohistochemical evaluation with proposed histopathological classification system. *J Comp Pathol.* 2024 Jul;212:42-50.
5. Kennedy PC, Cullen JM, Edwards JF, Goldschmidt MH, Larsen S, Munson L, Nielsen. *Histological classification of tumors of the genital system of domestic animals.* WHO, Washington, DC: Armed Forces Institute of Pathology; 1998.
6. MacLachlan NJ, Kennedy PC: Tumors of the genital system. In Meuten DJ: *Tumors in Domestic Animals.* 4th ed. Ames, IO: Iowa State Press;2002:547-573.
7. Matos ACHDS, Consalter A, Santos Batista BP, Fonseca ABM, Ferreira AMR, Leite JDS. Immunohistochemical expression of HER - 2 and Ki - 67 in granulosa cell tumor in bitches. *Reprod Dom Anim.* 2021;56(4):667–672
8. Oviedo-Peñata CA, Hincapie L, Riaño-Benavides C, Maldonado-Estrada JG. Concomitant Presence of Ovarian Tumors (Teratoma and Granulosa Cell Tumor), and Pyometra in an English Bulldog Female Dog: A Case Report. *Front Vet Sci.* 2020;6:500.
9. Patnaik AK, Greenlee PG. Canine Ovarian Neoplasms: A Clinicopathologic Study of 71 Cases, Including Histology of 12 Granulosa Cell Tumors. *Vet Pathol.* 1987;24(6):509–514.
10. Riccardi E, Greco V, Verganti S, Finazzi M. Immunohistochemical Diagnosis of Canine Ovarian Epithelial and Granulosa Cell Tumors. *J Vet Diagn Invest.* 2007;19(4):431–435
11. Rosa RB, Bianchi MV, Ribeiro PR, et al. Comparison of immunohistochemical profiles of ovarian germ cells in dysgerminomas of a captive maned wolf and domestic dogs. *J Ver Diagn Invest.* 2021;33(4):772–776.
12. Schlafer DH, Miller RB: Female genital system. In: Maxie MG, ed.. *Jubb, Kennedy, and Palmer's Pathology of Domestic Animals.* 5th ed. Philadelphia, PA: Elsevier Limited; 2007, vol 3: 450-456
13. Schlafer DH, Foster RA. Female Genital System. In: Maxie MG, ed. *Jubb, Kennedy & Palmer's Pathology of Domestic Animals.* Vol 3. 6th ed. St. Louis, MO: Elsevier; 2016:358-464.
14. Sforza M, Brachelente C, Lepri E, Mechelli L. Canine ovarian tumours: a retrospective study of 49 cases. *Vet Res Commun.* 2003;27:359–361.
15. Troisi A, Orlandi R, Vallesi E, Pastore S, Sforza M, Quartuccio M, Zappone V, Cristarella S, Polisca A. Clinical and ultrasonographic findings of ovarian tumours in bitches: A retrospective study. *Theriogenology.* 2023 Oct 15;210:227-233.
16. Walter B, Coelfen A, Jäger K, Reese S, Meyer-Lindenberg A, Aupperle-Lellbach H. Anti-Muellerian hormone concentration in bitches with histopathologically diagnosed ovarian tumours and cysts. *Reprod Domestic Animals.* 2018;53(3):784–792.
17. Yi C, Li L, Chen K, Lin S, Liu X. Expression of c-Kit and PDGFR $\alpha$  in epithelial ovarian tumors and tumor stroma. *Oncol Lett.* 2012 Feb;3(2):369-372.